Snowmelt Stimulates Ecosystem Respiration in Arctic Ecosystems

Running Title: Snowmelt and Carbon Respiration in the Arctic

Kyle A. Arndt[1,2], David Lipson[1], Josh Hashemi[1,2], Walter C. Oechel[1,3], and Donatella Zona[1,4]

Kyle Arndt ORCID iD: https://orcid.org/0000-0003-4158-2054

[1]Department of Biology, San Diego State University, San Diego, USA

[2]Department of Land, Air, and Water Resources, University of California at Davis, Davis, USA

[3]Department of Geography, University of Exeter, Exeter, UK

[4]Department of Plant and Animal Sciences, University of Sheffield, Sheffield, UK

Corresponding author: Kyle Arndt (karndt-w@sdsu.edu)

Abstract

Cold seasons in Arctic ecosystems are increasingly important to the annual carbon balance of these vulnerable ecosystems. Arctic winters are largely harsh and inaccessible leading historic data gaps during that time. Until recently, cold seasons have been assumed to have negligible impacts on the annual carbon balance but as data coverage increases and the Arctic warms, the cold season has been shown to account for over half of annual methane (CH_4) emissions and can offset summer photosynthetic carbon dioxide (CO_2) uptake. Freeze-thaw cycle dynamics play a critical role in controlling cold season CO_2 and CH_4 loss, but the relationship has not been extensively studied. Here we analyze freeze-thaw processes through in-situ CO_2 and CH_4 fluxes in conjunction with soil cores for physical structure and porewater samples for redox biogeochemistry. We find a movement of water towards freezing fronts in soil cores, leaving air spaces in soils, which allows for rapid infiltration of oxygen rich snowmelt in spring as shown by oxidized iron in porewater. The snowmelt period coincides with rising ecosystem respiration and can offset up to 41% of the summer CO_2 uptake. Our study highlights this important seasonal

process and shows spring greenhouse gas emissions are largely due to production from respiration instead of only bursts of stored gases. Further warming is projected to result in increases of snowpack and deeper thaws, which could increase this ecosystem respiration dominate snowmelt period causing larger greenhouse gas losses during spring.

Keywords: Snowmelt, Net Ecosystem Exchange, Methane Flux, Arctic Tundra, Spring, Freeze Thaw Cycle, Arctic Soil

30

MR. KYLE A ARNDT (Orcid ID : 0000-0003-4158-2054)
PROF. DONATELLA ZONA (Orcid ID : 0000-0002-0003-4839)

Article type : Primary Research Articles

Snowmelt Stimulates Ecosystem Respiration in Arctic Ecosystems

Running Title: Snowmelt and Carbon Respiration in the Arctic

Kyle A. Arndt[1,2], David Lipson[1], Josh Hashemi[1,2], Walter C. Oechel[1,3], and Donatella Zona[1,4]

Kyle Arndt ORCID iD: https://orcid.org/0000-0003-4158-2054

[1]Department of Biology, San Diego State University, San Diego, USA

[2]Department of Land, Air, and Water Resources, University of California at Davis, Davis, USA

[3]Department of Geography, University of Exeter, Exeter, UK

[4]Department of Plant and Animal Sciences, University of Sheffield, Sheffield, UK

Corresponding author: Kyle Arndt (karndt-w@sdsu.edu)

Abstract

Cold seasons in Arctic ecosystems are increasingly important to the annual carbon balance of these vulnerable ecosystems. Arctic winters are largely harsh and inaccessible leading historic data gaps during that time. Until recently, cold seasons have been assumed to have negligible impacts on the annual carbon balance but as data coverage increases and the Arctic warms, the cold season has been shown to account for over half of annual methane (CH_4) emissions and can offset summer photosynthetic carbon dioxide (CO_2) uptake. Freeze-thaw cycle dynamics play a critical role in controlling cold season CO_2 and CH_4 loss, but the relationship has not been extensively studied. Here we analyze freeze-thaw processes through in-situ CO_2 and CH_4 fluxes in conjunction with soil cores for physical structure and porewater samples for redox biogeochemistry. We find a movement of water towards freezing fronts in soil cores, leaving air spaces in soils, which allows for rapid infiltration of oxygen rich snowmelt in spring as shown by oxidized iron in porewater. The snowmelt period coincides with rising ecosystem respiration and can offset up to 41% of the summer CO_2 uptake. Our study highlights this important seasonal process and shows spring greenhouse gas emissions are largely due to production from respiration instead of only bursts of stored gases. Further warming is projected to result in increases of snowpack and deeper thaws, which could increase this ecosystem respiration dominate snowmelt period causing larger greenhouse gas losses during spring.

Keywords: Snowmelt, Net Ecosystem Exchange, Methane Flux, Arctic Tundra, Spring, Freeze Thaw Cycle, Arctic Soils

1 Introduction

Non-growing season carbon emissions (carbon dioxide (CO_2) and methane (CH_4)) have recently been emphasized for their critical role in the annual carbon balance, of Arctic ecosystems (Commane et al., 2017; Euskirchen et al., 2016; Natali et al., 2019; Oechel et al., 2014; Treat et al., 2018; Zona et al., 2016). Arctic tundra ecosystems have historically been an annual net sink of CO_2 (Oechel et al., 1993); however, some sites are now becoming annual net sources (Commane et al., 2017; Euskirchen et al., 2016; Oechel et al., 1993). Methane has been given increased attention as well given the Arctic is responsible for ~3% of global CH_4 emissions (Kirschke et al., 2013), with potential for increase given substantial climate changes (Schuur et al., 2015). Much of the carbon loss in the Arctic occurs over long winters, that comprise most of the year (typically around nine months), due to consistent winter emissions (Natali et al., 2019; Zona et al., 2016) coupled with occasional bursts (Mastepanov et al., 2013; Pirk et al., 2015; Raz-Yaseef et al., 2017).

Microbial respiration exponentially increases with temperature (Dunfield et al., 1993), therefore summer respiration rates are higher while soils are warm and thawed. However, summers are relatively short compared to the winter (including transitional shoulder seasons) and have photosynthetic activity that result in a net CO_2 sink during these months (Commane et al., 2017; Oechel et al., 1993; Oechel et al., 2014). In the fall shoulder season, a phenomenon known as the "zero-curtain" occurs where soil temperatures remain around 0°C during freezing (Hinkel et al., 2001). During the zero-curtain, CH_4 (Arndt et al., 2019a; Zona et al., 2016)and CO_2 (Commane et al., 2017) emission rates remain high, and can account for much of the annual carbon balance. Burst emissions have been observed as well which have raised fall CH_4 emissions from 37% of summer emissions to 92% due to the rapid release of gases from partially frozen soils (Mastepanov et al., 2013; Pirk et al., 2015). However, similar burst emissions have been observed during spring thaw, but fewer studies analyze the spring (Raz-Yaseef et al., 2017) leading to gaps in our knowledge of processes driving spring emissions.

CO_2 emissions during spring have been estimated to offset 46% of summer uptake (Raz-Yaseef et al., 2017). To better understand the processes leading to these high emissions during spring, soil freezing processes must be considered. During soil freeze, water migrates to top and bottom freezing fronts leaving air pockets in the active layer (Bing et al., 2015; Brown, 1967). Salts and ions are pushed out of freezing water fronts (Bing et al., 2015; Gray & Granger, 1985), which also occurs with gases. This helps explain how the zero-curtain becomes pressurized (Tagesson et al., 2012) as gases are forced out of solution into a small space. This pressure in the soil may be a leading cause of sometimes observed burst emissions (Mastepanov et al., 2013; Pirk et al., 2015). Air spaces remain in frozen soils until spring when oxygen rich snowmelt infiltrates soil (Yanai et al., 2011) and causes rapid warming due to convective heat transfer (Kane et al., 2001).

Microbial activity continues at below freezing temperatures, with sometimes variable temperature sensitivities (Mikan et al., 2002). There are notable differences in Arctic microbial community diversity between frozen and unfrozen soils (Buckeridge et al., 2013) causing variable dynamics of gas production and consumption. Conditions within the soil column including temperature (Mikan et al., 2002), nutrient availability (Schmidt & Lipson, 2004), and oxygen content (Buckeridge et al., 2013) all contribute to controlling microbial diversity and productivity. Of interest to our study, higher oxygen content would result in increased CO_2 production and stifled CH_4 production since aerobic respiration (produces CO_2) uses oxygen and methanogens are active in anerobic environments. Given the vulnerability of the large Arctic carbon pool (Schuur et al., 2015; Tarnocai, 2009), it is crucial to understand spring biogeochemical cycling to get a full picture what drives sometimes large emissions of CO_2 and CH_4. Accordingly, it is vital to understand the relative contribution various seasons have to the carbon budget to be able to better predict future scenarios as seasons dynamically change.

In this study we seek to understand biogeochemical processes, specifically the redox state in conjunction with CO_2 and CH_4 fluxes, causing the spring to sometimes be a relatively strong source of carbon. To do this, we use in-situ iron (Fe) pore water samples, soil cores, and eddy covariance (EC) tower carbon fluxes to explore (1) the process of spring soil oxidation , (2) oxidation controls of carbon fluxes, and (3) physical soil conditions leading to spring oxidation.

2 Materials and methods

2.1 Field site description

We conducted the study at five EC towers on the Alaska North Slope (Table 1, Fig. 1). EC sites consisted of US-Brw (Zona & Oechel, 2018d), US-Beo (Zona & Oechel, 2018b), and US-Bes (Zona & Oechel, 2018c), located outside of Utqiaġvik, Alaska; US-Atq (Zona & Oechel, 2018a), located near Atqasuk, Alaska about 100 km south of Utqiaġvik; and US-Ivo (Zona & Oechel, 2018e), located in Ivotuk, Alaska about 300 km south of Utqiaġvik. US-Brw is a moist upland tundra site and is dominated by graminoid grasses and lichens (Kwon et al., 2006). US-Beo is on polygonised tundra with a mix of wet and dry graminoids and sedges and US-Bes is in a drained lake basin dominated by sedges and Sphagnum mosses (Davidson et al., 2016). US-Atq is an inland polygonised site with tussock tundra, wet sedges, dwarf shrubs (Davidson et al., 2016), and sandy soils (Walker et al., 1989). US-Ivo is in the foothills of the Brooks Range on a gentle slope and is dominated by tussock tundra with a mossy layer between tussocks (Davidson et al., 2016).

2.2 Flux processing and instrumentation

Gas concentrations (CO_2 and CH_4) from the four northern sites were measured using the Los Gatos Research Fast Greenhouse Gas Analyzer (ABB Group, Zurich, CH) and a LI-COR® LI-7700 and LI-7200 were used for CH_4 and CO_2, respectively, at US-Ivo due to the lack of grid power at the site (Table 1). Three-dimensional wind speeds were measured using a uSonic-3 (METEK Meteorologische Messtechnik GmbH, DE) at US-Brw, a CSAT3 (Campbell Scientific®, Logan, UT) at US-Beo, US-Bes, and US-Atq, and a uSonic-3 Class A (METEK Meteorologische Messtechnik GmbH, DE) at US-Ivo. Flux data were recorded at 10 Hz on a CR3000 data logger (Campbell Scientific®, Logan, UT) at the northern four sites, and on a LI-7550 (LI-COR®, Lincoln NE, USA) at US-Ivo. A cross comparison between the various instruments ensures comparability of results across sites despite different instruments used (Goodrich et al., 2016).

Half-hourly net ecosystem exchange (NEE) and CH_4 fluxes were calculated using EddyPro® (LI-COR®, USA). When NEE is positive, it is a net source of CO_2 (emission dominate) to the atmosphere and when it is negative, a net sink (uptake dominate). Methane fluxes in this study were typically a net source and thus are referred to as emissions. A double rotation according to Wilczak et al. (2001) was applied to the three dimensional wind speed parameters. Covariance was maximized to compensate for time lags between vertical wind movements and gas concentrations. For US-Ivo, where the open path LI-7700 was used, a Webb, Pearman, and Leunig correction was applied (Webb et al., 1980). For the other sites with a closed path gas analyzer, an in-situ analytic correction was applied (Ibrom et al., 2007). High and low-pass filter effects were corrected for according to Moncrieff et al. (2005) and Moncrieff et al. (1997), respectively. Additional cleaning of half-hourly calculated fluxes were done following Arndt et al. (2019a). Initial gap filling of flux data was done using marginal distribution sampling following Wutzler et al. (2018) using the R package ReddyProc (Wutzler et al., 2019). This method uses look up windows to fill gaps and therefore does not work for long data gaps greater than 70 days. For longer data gaps, barring total power failure where meteorological data were not available, a neural network was used to impute fluxes using the R package neuralnet (Fritsch et al., 2019). See supporting information for model validation.

2.2.1 Meteorological data collection

Air temperature and humidity data were collected with HMP60s (Vaisala, Finland) and soil temperature using Type T thermocouples (Omega Engineering, USA). Snow depth was measured using SR50A sonic ranging sensors (Campbell Scientific, USA). Soil heat flux was measured with HFT3 soil heat flux plates (Campbell Scientific, USA). All metrics were scanned every 30 seconds and were recorded in 30-minute averages on a CR23X datalogger, except at US-Ivo where a CR3000 datalogger (Campbell Scientific, USA) was used. High resolution (thermocouples every 5 cm from 80 cm above the ground to a meter below ground) temperature data were used from Arndt et al. (2019b) to monitor the extent and timing of snowmelt convective heating in soils.

2.2.2 Seasonal determination

Spring was determined as the date between the onset of snowmelt and soil thawing at five cm depth. Soil heat flux was used to determine the start of snowmelt due to a sudden pulse of energy coinciding with snowmelt infiltrating soils. This was chosen as the most consistently prevalent variable across site-years. The first half hour period in May with a change in soil heat flux greater than 2 W m^{-2} was used to determine the start of snowmelt. This was compared visually with air temperature, snow depth, and soil temperature when possible to confirm signals, with consistent agreement, when data were available. Thaw was determined as the first day following snowmelt where the average daily soil temperature at 5 cm depth was greater than 2°C. This was used to ensure signals were not due to instrument error or a warm spell that subsequently refroze. The growing season started after thaw and ended when daily average NEE was positive, representing net source conditions. Even though some photosynthesis may still have occurred at this time, this gave the clearest idea of the strength of growing season sinks. For this study, fall and winter were lumped together as the cold season and was the period between the end of the growing season and the following spring. The beginning of the cold season was unable to be determined at US-Beo and US-Bes in 2016 and 2017, respectively. Therefore, the cold season start date from the opposite site (US-Beo or US-Bes) was used due to their proximity only about 500 meters apart. Similarly, US-Brw did not have soil temperature data in 2014 so the thaw date for US-Beo was used there. US-Beo did not have soil heat flux in 2014 so the melt date at US-Bes was used that site-year.

2.3 Sample collections

2.3.1 Soil core collection and preparation

Frozen soil cores were collected from the Alaska North Slope in April 2018 to understand the physical structure of the soil column including water and air pocket distribution. Cores were collected along a latitudinal gradient with sample names representing distance from the Arctic ocean (6km, 11km, 25km, and 100km) or were named after EC sites (US-Atq and US-Ivo) where sampling occurred (Fig. 1). Cores were wrapped in plastic and shipped frozen to the laboratory in San Diego, CA where they were stored at -30°C to retain physical structure. All cores were collected to a 40 cm depth and thus were 40 cm in length, except at US-Ivo where rocky soils prevented deeper sampling. Here cores were capped at 23 to 24 cm. Cores were cut with a band saw into five cm long cylinders, which were weighed before longitudinal subsamples of each section were removed and dried for >48 hours at 100°C to determine gravimetric water content. Bulk density was determined from the dry mass of each section per unit volume and used to calculate volumetric water content.

2.3.2 In-situ iron porewater

Soil porewater was sampled for two consecutive summers in 2010 and 2011 a few hundred meters northeast of the US-Bes EC tower site (Fig. 1b). Porewater was sampled repeatedly using Rhizon soil water samplers, type MOM, installed from 0-10 cm (Lipson et al., 2013; Miller et al., 2015). Samples were preserved with a drop of 1M HCl and shipped to the laboratory in San

Diego, CA for analysis of total Fe and Fe^{2+} using the 1,10-phenanthroline method (Lipson et al., 2010).

2.4 Statistical analyses

Soil water content trends were assessed using a mixed effects model using the nlme R package (Pinheiro et al., 2018) and the MuMIn R package (Barton, 2019) was used to assess correlation coefficients. Reduction of Fe over the course of two growing season was assessed using Mann Kendall trend analysis sensitive to time-series data according to Yue et al. (2002) using the zyp R package (Bronaugh & Werner, 2019). This properly accounts for autocorrelation in timeseries data. Gap filled fluxes of CO_2 and CH_4 were used to assess carbon budgets. US-Beo 2017, US-Bes 2016, and US-Atq 2016 and 2017 were not included in analysis of the spring budget due to no real data coverage in those site years. Data coverage during seasons surrounding the growing season ranged from 44.5% to 65.6% (see supporting information). All data analyses were performed using R v. 3.5.2 (R Core Team, 2018) and visuals were created using ggplot2 (Hadley, 2016), ggmap (Kahle & Wickham, 2013), cowplot (Wilke, 2019), and RColorBrewer (Neuwirth, 2014) R packages.

3 Results

3.1 Water movement during freezing

Soil cores collected after full freezing in April 2018 show signs of water movement from the core center (around 20 cm depth) to the surface and bottom (near 40 cm depth) of the active layer. The mixed effects model of soil water content as a function of depth showed a significant polynomial trend ($y = 78.3 + 39.4x + 53.3x^2$, $n = 47$, $P = 0.01$, $R^2 = 0.22$, Fig. 2a) showing that water was concentrated at the top and bottom of soil cores leaving airspaces in the middle. All sites followed the trend except for US-Ivo, where the depth of soil cores was limited to 25 cm due to sampling difficulty in rocky soils (Fig. 2a). Values above 100% were possible due to ice lensing effects.

3.2 Redox cycles

In-situ Fe in pore water showed reduction occurred over the growing season leading to reduced Fe in soils by the fall. Pore water Fe was oxidized before the beginning of the following growing season (Fig. 2b). Fe became significantly reduced in a logarithmic pattern where 2010 (y = 1.4ln(x) – 7.0, R^2 = 0.63, P = 0.04) progressed slower than 2011 (y = 2.8ln(x) – 14.4, R^2 = 0.79, P = 0.01).

3.3 Snowmelt signals

Several meteorological variables lined up with spring snowmelt across field sites. At snowmelt onset, a sudden ground heat flux pulse was observed (Fig. 3a). At the same time, soil temperatures quickly warmed to 0°C until complete thaw. As melting progressed, soil heat flux remained steadily near 10 W m^{-2} with occasional pulses aligning with more rapid snowmelt events. During snowmelt, steady emissions of CO_2 were observed with a clear rise at the onset of snowmelt. Methane emissions rose slowly beginning with snowmelt and jumped up once soils were thawed and ecosystems became photosynthesis dominated.

High resolution soil temperature profiles showed convective heat transfer in the soil column during snowmelt (Fig. 4). Snow depth can be seen in these data around 50 cm above the soil surface where temperatures pause at or below 0°C with diurnal fluctuations seen above. On days where air temperatures approached 10°C, rapid melting occurred, and pulses were seen in the soil showing convective warming due to snowmelt infiltrating soil. Snowmelt effects lasted several days with sometimes subsequent cooling as soils refroze. Once air temperatures reached consistent daily highs above 5°C, steady snowmelt occurred causing steady convective heating and impacted soils down to a meter depth.

3.4 Spring contribution to the carbon balance

Spring ecosystem respiration offset between -4.5% and 41% of the growing season CO_2 sink depending on the year and site (Fig. 5). Negative values indicate a spring sink for that site-year. US-Atq and US-Ivo sometimes showed a net sink during spring snowmelt and ranged from 4.3 g C-CO_2 m^{-2} to 4.5 g C-CO_2 m^{-2}, in 2015 and 2017, respectively. Summer growing season NEE was always a net sink of CO_2 taking in between 111.3 g C-CO_2 m^{-2} and 30.3 g C-CO_2 m^{-2}. The cold season showed a source of CO_2 across sites ranging between 1.5 g C-CO_2 m^{-2} and 106.2 g C-CO_2 m^{-2}. Spring was a small portion of the annual CH_4 budget at each of the five sites ranging between 0.01 g C-CH_4 m^{-2} to 0.58 g C-CH_4 m^{-2}. This is compared to the growing season which ranged from 0.45 g C-CH_4 m^{-2} to 2.25 g C-CH_4 m^{-2} and cold season emissions ranging from 0.36

g C-CH_4 m^{-2} to 4.43 g C-CH_4 m^{-2}. On average, spring ecosystem respiration offset 10.2 ± 3.5% of the summer CO_2 sink and contributed 6.2 ± 2.3% of annual CH_4 emissions.

4 Discussion

We analyzed the freeze-thaw effects on the carbon balance of Arctic ecosystems and found the spring creates unique conditions supporting the onset of ecosystem respiration during snowmelt. Water migrates up and down to freezing fronts during soil freezing (Bing et al., 2015; Brown, 1967). This creates air pockets, even in inundated soils, as we saw in our soil cores in agreement with recent studies using CT scans of soil cores collected near Utqiaġvik (Raz-Yaseef et al., 2017). Due to gases being pushed out of solution during freezing, this could aid in creating pressurized gas layers in soils after the surface has frozen (Tagesson et al., 2012). As soil gas concentrations in Arctic soils are high during the summer and tail off in August (Abbott & Jones, 2015), concentrations increase during fall due to the frozen surface trapping gases (Raz-Yaseef et al., 2017). This gas can then be released through bursts or diffusional processes through vegetation (Kwon et al., 2017). These air gaps leave space for the spring snowmelt flush that we suggest ramps up spring ecosystem respiration due to the introduction of oxygen and rapid warming (Fig. 6). If spring emissions were only due to the release of stored gases, we would expect sudden emissions up thawing and tailing off until production began, however, we noticed a consistent ramping up of emissions.

During snowmelt, soil fissures are common (Raz-Yaseef et al., 2017) and we suggest snowmelt enters soil air spaces during thaw. We suggest snowmelt infiltration can bring oxygen into anaerobic soils supported by the in-situ Fe samples showing reduction over the growing season with almost fully oxidized Fe in soils following snowmelt. As ice cracks over the winter period are scarce (Raz-Yaseef et al., 2017; Sturtevant et al., 2012; Tagesson et al., 2012) and surface ice creates a barrier to gas exchange (Elberling & Brandt, 2003), we suggest the observed oxidation is due to the oxygen rich snowmelt infiltrating soils. Further, the lack of burst emissions emphasize the rarity of large-scale exchanges over the cold season. Even during the growing season, oxygen diffusion is slow and oxygen is quickly consumed in soils (Elberling et al., 2011), so large scale soil oxidation is likely not occurring in the winter with the extra barriers of snow and ice. When oxygen is quickly introduced into the soil column by snowmelt, it likely aids biogeochemical cycling as seen by the rise of ecosystem respiration rates.

Physical processes of freezing and thawing in soils can help to understand greenhouse gas fluxes at this time. We found that the spring emissions can impact the balance of CO_2 and CH_4 from Arctic tundra ecosystems. The one site (US-Ivo) that did not have clear water migration in the soil core, also did not show a prominent respiration increase; however, the core sampling depth was low in comparison to the active layer depth (see supporting information) and missed the middle of the active layer. If air pockets are not created in the soil, the site would not be primed for a snowmelt flush further suggesting the link between respiration and snowmelt.

Previous studies have found spring CO_2 emissions to offset as much as 47% of summer uptake, close to our maximum 41% observed at US-Brw, however the study attributed the release to bursts of gases stored over winter (Raz-Yaseef et al., 2017). These bursts are similar to burst emissions seen in other studies of the fall freeze-in period where large sudden emissions can make up much of the carbon balance (Mastepanov et al., 2013; Pirk et al., 2015; Tagesson et al., 2012). However, we suggest there is more to the process than bursts of gasses stored over winter. The introduction of oxygen into the soil column and rapid warming during spring thaw, we suggest kickstarts ecosystem respiration by creating supporting conditions. Oxygen aids CO_2 production but inhibits CH_4 production evidenced by our EC data where CO_2 exhibits a steady emission rate while spring CH_4 slowly ramps up. Methane produced at depth may be consumed by methanotrophs in upper soil layers taking advantage of oxygen rich snowmelt therefore converting the CH_4 to CO_2. Further, Fe reduction likely adds to observed CO_2 emissions because the Fe reduction process can comprise 40-45% of respiration from these ecosystems (Lipson et al., 2013).

Microbial communities have been shown to be active during zero-curtain conditions and the colder winter period (Schimel & Mikan, 2005). There is a prominent shift in microbial communities during the spring thaw showing new growth of microbes at this time albeit nutrient limited (Buckeridge et al., 2013). Nutrient limitations may explain why CH_4 flux rates jump after thaw when photosynthesis begins, as photosynthates and plant mediated transport can be important controls of CH_4 emissions (Dorodnikov et al., 2011). We suggest that the introduction of oxygen may aid microbial community change and increase microbial activity.

Climate predictions for Arctic ecosystems show warming winters (Bekryaev et al., 2010) and increased winter precipitation (Liu et al., 2012; Screen & Simmonds, 2011) which could extend the duration of snowmelt therefore extending net source conditions. Warmer springs may also cause more rapid snowmelt and an earlier start to the growing season but the extent to which the growing season can advance is limited by photoperiod and moisture (Ernakovich et al., 2014). This means that even if snow continues to melt earlier, photosynthesis will become limited by other factors supporting increased periods of carbon loss. Studies suggest that Arctic vegetation has not reached maximum photosynthetic capacity and may increase uptake in the future (Rogers et al., 2017), but with increasing zero-curtain (Arndt et al., 2019a; Commane et al., 2017) and cold season emissions (Natali et al., 2019), the carbon balance of Arctic ecosystems may continue to shift to net source conditions.

5 Conclusions

Cold seasons in the Arctic are having an increasing importance on the annual carbon balance of Arctic tundra ecosystems. While long-term data records are coming to fruition, these ecosystems are complicated, and many controlling variables are not accounted for making model predictions and estimates uncertain. Here we show snowmelt may introduce oxygen into soils and cause rapid warming kickstarting ecosystem respiration. Spring can negate almost half of summer CO2 uptake from our sites and it is crucial to understand the underlying processes to be able to better predict carbon dynamics in a fast-changing climate. It has largely been assumed that most winter emissions of CO_2 and CH_4 are through bursts, but we suggest there are conditions that support consistent production and emissions of gases. With the vast stores of organic carbon in Arctic soils and a quickly changing climate, continued research into poorly understood seasons is critical to gaining an understanding on the future of the global climate.

Acknowledgments

This work was funded by the National Science Foundation (NSF) Office of Polar Programs (OPP) awarded to DZ, WCO, and DL (award number 1204263, 1702797, and 1712774) with additional logistical support funded by the NSF Office of Polar Programs, by the NASA ABoVE Program (NNX16AF94A) awarded to WCO and DZ, by NOAA EPP (award number NA16SEC4810008) to WCO, from the European Union's Horizon 2020 research and innovation program under grant agreement No. 629727890 to WCO and DZ, and from the Natural Environment Research Council (NERC) UAMS Grant (NE/P002552/1) to WCO and

DZ. The data that support the findings of this study are openly available from the following sources. EC tower flux data are available from Ameriflux, DOIs are as follows: US-Brw, http://dx.doi.org/10.17190/AMF/1246041; US-Atq, http://dx.doi.org/10.17190/AMF/1246029; US-Ivo, http://dx.doi.org/10.17190/AMF/1246067. US-Bes EC data is available from ameriflux at the following URL, https://ameriflux.lbl.gov/sites/siteinfo/US-Bes. US-Beo data is available from Ameriflux at the following URL, https://ameriflux.lbl.gov/sites/siteinfo/US-Bes. High resolution soil temperature data is available from the NSF Arctic Data Center, doi:10.18739/A25X25C75. Porewater data are available from the NSF Arctic Data Center, doi:10.18739/A2RW4G and doi:10.18739/A2DP62. Thaw depth and water table data are available from the NSF Arctic Data Center, doi:10.18739/A26H4CQ8J. Soil core data are available from the NSF Arctic Data Center, doi:10.18739/A2PK0723G. This research was conducted on land owned by the Ukpeaġvik Inupiat Corporation (UIC) whom we thank for their support. Authors also thank the R developing team (R core team, Vienna, Austria) in creating the open source R statistical software. The authors declare no conflicts of interest.

References

Abbott, B. W., & Jones, J. B. (2015). Permafrost collapse alters soil carbon stocks, respiration, CH4 , and N2O in upland tundra. Glob Chang Biol, 21(12), 4570-4587. doi:10.1111/gcb.13069

Arndt, K. A., Oechel, W. C., Goodrich, J. P., Bailey, B. A., Kalhori, A., Hashemi, J., . . . Zona, D. (2019a). Sensitivity of Methane Emissions to Later Soil Freezing in Arctic Tundra Ecosystems. Journal of Geophysical Research: Biogeosciences, 124(8), 2595-2609. doi:10.1029/2019jg005242

Arndt, K. A., Zona, D., Hashemi, J., Kalhori, A. A. M., & Oechel, W. (2019b). High resolution temperature profiles along a latitudinal gradient near Utqiagvik, Atqasuk, and Ivotuk Alaska from 2016-2019. Retrieved from: https://doi.org/10.18739/A25X25C75

Barton, K. (2019). MuMIn: Multi-Model Inference.

Bekryaev, R. V., Polyakov, I. V., & Alexeev, V. A. (2010). Role of Polar Amplification in Long-Term Surface Air Temperature Variations and Modern Arctic Warming. Journal of Climate, 23(14), 3888-3906. doi:10.1175/2010jcli3297.1

Bing, H., He, P., & Zhang, Y. (2015). Cyclic freeze–thaw as a mechanism for water and salt migration in soil. Environmental Earth Sciences, 74(1), 675-681. doi:10.1007/s12665-015-4072-9

Bronaugh, D., & Werner, A. (2019). zyp: Zhang + Yue-Pilon Trends Package.

Brown, J. (1967). Tundra Soils Formed over Ice Wedges, Northern Alaska1. Soil Science Society of America Journal, 31(5), 686-691. doi:10.2136/sssaj1967.03615995003100050022x

Buckeridge, K. M., Banerjee, S., Siciliano, S. D., & Grogan, P. (2013). The seasonal pattern of soil microbial community structure in mesic low arctic tundra. Soil Biology and Biochemistry, 65, 338-347. doi:10.1016/j.soilbio.2013.06.012

Commane, R., Lindaas, J., Benmergui, J., Luus, K. A., Chang, R. Y., Daube, B. C., . . . Wofsy, S. C. (2017). Carbon dioxide sources from Alaska driven by increasing early winter respiration from Arctic tundra. Proc Natl Acad Sci U S A, 114(21), 5361-5366. doi:10.1073/pnas.1618567114

Davidson, S. J., Santos, M. J., Sloan, V. L., Watts, J. D., Phoenix, G. K., Oechel, W. C., & Zona, D. (2016). Mapping Arctic Tundra Vegetation Communities Using Field Spectroscopy and Multispectral Satellite Data in North Alaska, USA. Remote Sensing, 8(12). doi:ARTN 978 10.3390/rs8120978

Dorodnikov, M., Knorr, K. H., Kuzyakov, Y., & Wilmking, M. (2011). Plant-mediated CH4 transport and contribution of photosynthates to methanogenesis at a boreal mire: a 14C pulse-labeling study. Biogeosciences, 8(8), 2365-2375. doi:10.5194/bg-8-2365-2011

Dunfield, P., Knowles, R., Dumont, R., & Moore, T. R. (1993). Methane production and consumption in temperate and subarctic peat soils: Response to temperature and pH. Soil Biology and Biochemistry, 25(3), 321-326. doi:https://doi.org/10.1016/0038-0717(93)90130-4

Elberling, B., Askaer, L., Jørgensen, C. J., Joensen, H. P., Kühl, M., Glud, R. N., & Lauritsen, F. R. (2011). Linking Soil O2, CO2, and CH4Concentrations in a Wetland Soil: Implications for CO2and CH4Fluxes. Environmental Science & Technology, 45(8), 3393-3399. doi:10.1021/es103540k

Elberling, B., & Brandt, K. K. (2003). Uncoupling of microbial CO2 production and release in frozen soil and its implications for field studies of arctic C cycling. Soil Biology and Biochemistry, 35(2), 263-272. doi:https://doi.org/10.1016/S0038-0717(02)00258-4

Ernakovich, J. G., Hopping, K. A., Berdanier, A. B., Simpson, R. T., Kachergis, E. J., Steltzer, H., & Wallenstein, M. D. (2014). Predicted responses of arctic and alpine ecosystems to altered seasonality under climate change. Glob Chang Biol, 20(10), 3256-3269. doi:10.1111/gcb.12568

Euskirchen, E. S., Bret-Harte, M. S., Shaver, G. R., Edgar, C. W., & Romanovsky, V. E. (2016). Long-Term Release of Carbon Dioxide from Arctic Tundra Ecosystems in Alaska. Ecosystems, 20(5), 960-974. doi:10.1007/s10021-016-0085-9

Fritsch, S., Guenther, F., & Wright, M. N. (2019). neuralnet: Training of Neural Networks (Version R package version 1.44.2). Retrieved from https://CRAN.R-project.org/package=neuralnet

Goodrich, J. P., Oechel, W. C., Gioli, B., Moreaux, V., Murphy, P. C., Burba, G., & Zona, D. (2016). Impact of different eddy covariance sensors, site set-up, and maintenance on the annual balance of CO 2 and CH 4 in the harsh Arctic environment. Agricultural and Forest Meteorology, 228-229, 239-251. doi:10.1016/j.agrformet.2016.07.008

Gray, D., & Granger, R. (1985). In situ measurement of moisture and salt movement in frozen soils. Canadian Journal of Earth Sciences, 23, 696-704. doi:10.1139/e86-069

Hadley, W. (2016). ggplot2: Elegant Graphics for Data Analysis. New York: Springer-Verlag. Retrieved from https://ggplot2.tidyverse.org

Hinkel, K. M., Paetzold, F., Nelson, F. E., & Bockheim, J. G. (2001). Patterns of soil temperature and moisture in the active layer and upper permafrost at Barrow, Alaska: 1993–1999. Global and Planetary Change, 29(3), 293-309. doi:https://doi.org/10.1016/S0921-8181(01)00096-0

Ibrom, A., Dellwik, E., Flyvbjerg, H., Jensen, N. O., & Pilegaard, K. (2007). Strong low-pass filtering effects on water vapour flux measurements with closed-path eddy correlation systems. Agricultural and Forest Meteorology, 147(3), 140-156. doi:https://doi.org/10.1016/j.agrformet.2007.07.007

Kahle, D., & Wickham, H. (2013). ggmap: Spatial Visualization with ggplot2. The R Journal, 5(1), 144 - 161.

Kane, D. L., Hinkel, K. M., Goering, D. J., Hinzman, L. D., & Outcalt, S. I. (2001). Non-conductive heat transfer associated with frozen soils. Global and Planetary Change, 29(3), 275-292. doi:https://doi.org/10.1016/S0921-8181(01)00095-9

Kirschke, S., Bousquet, P., Ciais, P., Saunois, M., Canadell, J. G., Dlugokencky, E. J., . . . Zeng, G. (2013). Three decades of global methane sources and sinks. Nature Geoscience, 6(10), 813-823. doi:10.1038/ngeo1955

Kwon, H.-J., Oechel, W. C., Zulueta, R. C., & Hastings, S. J. (2006). Effects of climate variability on carbon sequestration among adjacent wet sedge tundra and moist tussock tundra ecosystems. Journal of Geophysical Research, 111(G3). doi:10.1029/2005jg000036

Kwon, M. J., Beulig, F., Ilie, I., Wildner, M., Kusel, K., Merbold, L., . . . Gockede, M. (2017). Plants, microorganisms, and soil temperatures contribute to a decrease in methane fluxes on a drained Arctic floodplain. Glob Chang Biol, 23(6), 2396-2412. doi:10.1111/gcb.13558

Lipson, D. A., Jha, M., Raab, T. K., & Oechel, W. C. (2010). Reduction of iron (III) and humic substances plays a major role in anaerobic respiration in an Arctic peat soil. Journal of Geophysical Research, 115. doi:10.1029/2009jg001147

Lipson, D. A., Raab, T. K., Goria, D., & Zlamal, J. (2013). The contribution of Fe(III) and humic acid reduction to ecosystem respiration in drained thaw lake basins of the Arctic Coastal Plain. Global Biogeochemical Cycles, 27(2), 399-409. doi:10.1002/gbc.20038

Liu, J., Curry, J. A., Wang, H., Song, M., & Horton, R. M. (2012). Impact of declining Arctic sea ice on winter snowfall. Proc Natl Acad Sci U S A, 109(11), 4074-4079. doi:10.1073/pnas.1114910109

Mastepanov, M., Sigsgaard, C., Tagesson, T., Ström, L., Tamstorf, M. P., Lund, M., & Christensen, T. R. (2013). Revisiting factors controlling methane emissions from high-Arctic tundra. Biogeosciences, 10(7), 5139-5158. doi:10.5194/bg-10-5139-2013

Mikan, C. J., Schimel, J. P., & Doyle, A. P. (2002). Temperature controls of microbial respiration in arctic tundra soils above and below freezing. Soil Biology and Biochemistry, 34(11), 1785-1795. doi:https://doi.org/10.1016/S0038-0717(02)00168-2

Miller, K. E., Lai, C.-T., Friedman, E. S., Angenent, L. T., & Lipson, D. A. (2015). Methane suppression by iron and humic acids in soils of the Arctic Coastal Plain. Soil Biology and Biochemistry, 83, 176-183. doi:10.1016/j.soilbio.2015.01.022

Moncrieff, J., Clement, R., Finnigan, J., & Meyers, T. (2005). Averaging, Detrending, and Filtering of Eddy Covariance Time Series. In X. Lee, W. Massman, & B. Law (Eds.), Handbook of Micrometeorology: A Guide for Surface Flux Measurement and Analysis (pp. 7-31). Dordrecht: Springer Netherlands.

Moncrieff, J., Massheder, J. M., de Bruin, H., Elbers, J., Friborg, T., Heusinkveld, B., . . . Verhoef, A. (1997). A system to measure surface fluxes of momentum, sensible heat, water vapour and carbon dioxide. Journal of Hydrology, 188-189, 589-611. doi:https://doi.org/10.1016/S0022-1694(96)03194-0

Natali, S. M., Watts, J. D., Rogers, B. M., Potter, S., Ludwig, S. M., Selbmann, A.-K., . . . Zona, D. (2019). Large loss of CO_2 in winter observed across the northern permafrost region. Nature Climate Change, 9(11), 852-857. doi:10.1038/s41558-019-0592-8

Neuwirth, E. (2014). RColorBrewer: ColorBrewer Palettes (Version R package version 1.1-2). Retrieved from https://CRAN.R-project.org/package=RColorBrewer

Oechel, W. C., Hastings, S. J., Vourlrtis, G., Jenkins, M., Riechers, G., & Grulke, N. (1993). Recent change of Arctic tundra ecosystems from a net carbon dioxide sink to a source. Nature, 361(6412), 520-523. doi:10.1038/361520a0

Oechel, W. C., Laskowski, C. A., Burba, G., Gioli, B., & Kalhori, A. A. M. (2014). Annual patterns and budget of CO_2flux in an Arctic tussock tundra ecosystem. Journal of Geophysical Research: Biogeosciences, 119(3), 323-339. doi:10.1002/2013jg002431

Pinheiro, J., Bates, D., DebRoy, S., Sarkar, D., & Team, R. C. (2018). nlme: Linear and Nonlinear Mixed Effects Models.

Pirk, N., Santos, T., Gustafson, C., Johansson, A. J., Tufvesson, F., Parmentier, F.-J. W., . . . Christensen, T. R. (2015). Methane emission bursts from permafrost environments during autumn freeze-in: New insights from ground-penetrating radar. Geophysical Research Letters, 42(16), 6732-6738. doi:10.1002/2015gl065034

R Core Team. (2018). R: A Language and Environment for Statistical Computing. In.

Raz-Yaseef, N., Torn, M. S., Wu, Y., Billesbach, D. P., Liljedahl, A. K., Kneafsey, T. J., . . . Wullschleger, S. D. (2017). Large CO_2 and CH_4 emissions from polygonal tundra during spring thaw in northern Alaska. Geophysical Research Letters, 44(1), 504-513. doi:10.1002/2016gl071220

Rogers, A., Serbin, S. P., Ely, K. S., Sloan, V. L., & Wullschleger, S. D. (2017). Terrestrial biosphere models underestimate photosynthetic capacity and CO_2 assimilation in the Arctic. New Phytol, 216(4), 1090-1103. doi:10.1111/nph.14740

Schimel, J. P., & Mikan, C. (2005). Changing microbial substrate use in Arctic tundra soils through a freeze-thaw cycle. Soil Biology and Biochemistry, 37(8), 1411-1418. doi:10.1016/j.soilbio.2004.12.011

Schmidt, S. K., & Lipson, D. A. (2004). Microbial growth under the snow: Implications for nutrient and allelochemical availability in temperate soils. Plant and Soil, 259(1), 1-7. doi:10.1023/B:PLSO.0000020933.32473.7e

Schuur, E. A., McGuire, A. D., Schadel, C., Grosse, G., Harden, J. W., Hayes, D. J., . . . Vonk, J. E. (2015). Climate change and the permafrost carbon feedback. Nature, 520(7546), 171-179. doi:10.1038/nature14338

Screen, J. A., & Simmonds, I. (2011). Declining summer snowfall in the Arctic: causes, impacts and feedbacks. Climate Dynamics, 38(11-12), 2243-2256. doi:10.1007/s00382-011-1105-2

Sturtevant, C. S., Oechel, W. C., Zona, D., Kim, Y., & Emerson, C. E. (2012). Soil moisture control over autumn season methane flux, Arctic Coastal Plain of Alaska. Biogeosciences, 9(4), 1423-1440. doi:10.5194/bg-9-1423-2012

Tagesson, T., Mölder, M., Mastepanov, M., Sigsgaard, C., Tamstorf, M. P., Lund, M., . . . Ström, L. (2012). Land-atmosphere exchange of methane from soil thawing to soil freezing in a high-Arctic wet tundra ecosystem. Global Change Biology, 18(6), 1928-1940. doi:10.1111/j.1365-2486.2012.02647.x

Tarnocai, C. (2009). The Impact of Climate Change on Canadian Peatlands. Canadian Water Resources Journal / Revue canadienne des ressources hydriques, 34(4), 453-466. doi:10.4296/cwrj3404453

Treat, C. C., Bloom, A. A., & Marushchak, M. E. (2018). Nongrowing season methane emissions-a significant component of annual emissions across northern ecosystems. Glob Chang Biol, 24(8), 3331-3343. doi:10.1111/gcb.14137

Walker, D. A., Binnian, E. F., Evans, B. M., Lederer, N. D., Nordstrand, E. A., & Webber, P. J. (1989). Terrain, vegetation, and landscape evolution of the R4D research site, Brooks Range Foothills, Alaska. Holarctic Ecology, 12(3), 238-261.

Webb, E. K., Pearman, G. I., & Leuning, R. (1980). Correction of flux measurements for density effects due to heat and water vapour transfer. Quarterly Journal of the Royal Meteorological Society, 106(447), 85-100. doi:doi:10.1002/qj.49710644707

Wilczak, J. M., Oncley, S. P., & Stage, S. A. (2001). Sonic Anemometer Tilt Correction Algorithms. Boundary-Layer Meteorology, 99(1), 127-150. doi:10.1023/a:1018966204465

Wilke, C. O. (2019). cowplot: Streamlined Plot Theme and Plot Annotations for 'ggplot2' (Version R package version 1.0.0). Retrieved from https://CRAN.R-project.org/package=cowplot

Wutzler, T., Lucas-Moffat, A., Migliavacca, M., Knauer, J., Sickel, K., Šigut, L., . . . Reichstein, M. (2018). Basic and extensible post-processing of eddy covariance flux data with REddyProc. Biogeosciences, 15(16), 5015-5030. doi:10.5194/bg-15-5015-2018

Wutzler, T., Reichstein, M., Moffat, A. M., & Migliavacca, M. (2019). REddyProc: Post Processing of (Half-)Hourly Eddy-Covariance Measurements.

Yanai, Y., Hirota, T., Iwata, Y., Nemoto, M., Nagata, O., & Koga, N. (2011). Accumulation of nitrous oxide and depletion of oxygen in seasonally frozen soils in northern Japan – Snow cover manipulation experiments. Soil Biology and Biochemistry, 43(9), 1779-1786. doi:10.1016/j.soilbio.2010.06.009

Yue, S., Pilon, P., Phinney, B., & Cavadias, G. (2002). The influence of autocorrelation on the ability to detect trend in hydrological series. Hydrological Processes, 16(9), 1807-1829. doi:10.1002/hyp.1095

Zona, D., Gioli, B., Commane, R., Lindaas, J., Wofsy, S. C., Miller, C. E., . . . Oechel, W. C. (2016). Cold season emissions dominate the Arctic tundra methane budget. Proc Natl Acad Sci U S A, 113(1), 40-45. doi:10.1073/pnas.1516017113

Zona, D., & Oechel, W. (2018a). Ameriflux US-Atq Atqasuk. Retrieved from: http://dx.doi.org/10.17190/AMF/1246029

Zona, D., & Oechel, W. (2018b). Ameriflux US-Beo Barrow Environmental Observatory.

Zona, D., & Oechel, W. (2018c). Ameriflux US-Bes Biocomplexity Experiment South.

Zona, D., & Oechel, W. (2018d). AmeriFlux US-Brw Barrow. Retrieved from: http://dx.doi.org/10.17190/AMF/1246041

Zona, D., & Oechel, W. (2018e). AmeriFlux US-Ivo Ivotuk. Retrieved from: http://dx.doi.org/10.17190/AMF/1246067

Tables

Table 1: Summary of the eddy covariance (EC) towers used in this study. EC towers are on a latitudinal gradient from north to south and represent various Arctic tundra ecosystems. Air temperature (Air T.) is the mean ± standard error of the annual temperature at EC sites. See supporting information for additional meteorological observations.

Site	Latitude	Longitude	CO_2 Analyzer	CH_4 Analyzer	Sonic Anemometer	Air T. (°C)
US-Brw	71.322	-156.609	LGR FGGA	LGR FGGA	Metek uSonic3	-8.93 ± 3.38
US-Beo	71.281	-156.612	LGR FGGA	LGR FGGA	CSAT 3	-8.93 ± 3.43
US-Bes	71.281	-156.596	LGR FGGA	LGR FGGA	CSAT 3	-9.56 ± 3.47
US-Atq	70.470	-157.409	LGR FGGA	LGR FGGA	CSAT 3	-9.07 ± 3.70
US-Ivo	68.486	-155.750	LI-7200	LI-7700	Metek uSonic3 USA-1	-8.09 ± 3.72

Figure Captions

Figure 1: Maps of the location of the eddy covariance (EC) tower sites and pore water (PW) and core sample locations. Tower are labeled by their Ameriflux designations and core samples as a distance from the Arctic Ocean. Soil cores sampled near towers are suffixed with a "-C" after the EC tower site name. Map data are from Google with imagery from TerraMetrics (a and b), and Maxar Technologies (c and d).

Figure 2: (a) Water filled pore space in soil cores collected April 2018 at field sites. Results showed water migrating to freezing fronts leaving airspace in soils. (b) Soil pore water reduced iron (Fe^{2+}) over total iron (Fe) ratio showed significant reduction of Fe over the course of the growing season in 2010 and 2011. Fe was nearly fully oxidized in the spring. Points and error bars represent the mean and standard error.

Figure 3: Representative meteorological variables used to assess spring carbon release at US-Brw in 2015. (a) Soil heat flux peaks marked snowmelt followed by steady energy entering soils. Soil temperatures rose to 0°C and air temperatures reached above freezing temperatures at the same time. (b) Snowmelt began May 16th at this site-year lined up with metrics in panel a. NEE rose from low winter source conditions showing signs of consistent ecosystem respiration. (c) Methane emissions slowly rose at the same time and fully rise to peak summer emissions after soil thaw.

Figure 4: Temperatures from a meter below the soil surface to 80cm above. Data were from a low center polygon at the US-Atq site in spring 2017. (a) The cyan color shows temperatures near 0°C showing snow above the surface during thawing. Diurnal cycles of air temperatures were seen and convective heat warming soils quickly to 0°C as snow melts. (b) Zoomed image of the red box in panel a, a different temperature scale was used to better show heat penetration in soil highlighted by white arrows.

Figure 5: Sums of gap filled net ecosystem exchange (NEE) and methane (CH_4) emissions from the five tower sites. Asterisks represent the annual sum for NEE and CH_4 with positive values indicating a source, and negative indicating uptake. The growing season is a consistent sink across sites with the cold season

always being a net source of carbon dioxide (CO_2). Spring contributed little to CH_4 emissions with the growing season and winter making up the bulk of the balance.

Figure 6: Seasonal phase changes in the soil profile leading to oxygenation and convective heating in spring. In late summer, the soil profile is saturated, growing anoxic with depth. Small circles represent dissolved gases. During the zero-curtain period in the fall, water migrates to the upper and lower freezing fronts and gases are driven out of solution, leading to unsaturated voids in the middle of the profile in winter. In spring, snowmelt can penetrate these pockets, bringing oxygen to lower layers and causing rapid warming.

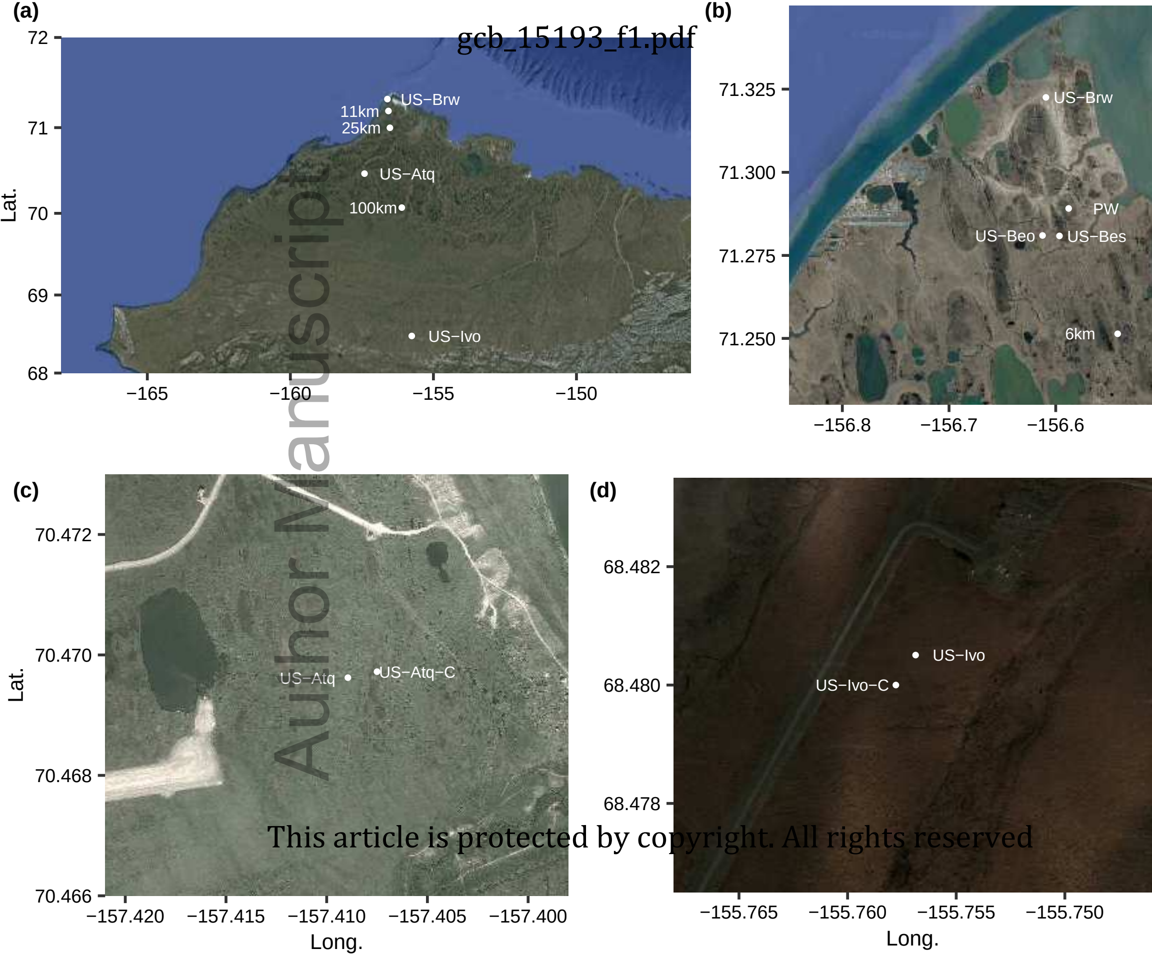
(a)
72
71
70
69
68
Lat.
US−Brw
11km
25km
US−Atq
100km
US−Ivo
−165
−160
−155
−150
(b)
71.325
71.300
71.275
71.250
US−Brw
PW
US−Beo
US−Bes
6km
−156.8
−156.7
−156.6
(c)
70.472
70.470
70.468
70.466
Lat.
US−Atq
US−Atq−C
−157.420
−157.415
−157.410
−157.405
−157.400
Long.
(d)
68.482
68.480
68.478
US−Ivo
US−Ivo−C
−155.765
−155.760
−155.755
−155.750
Long.

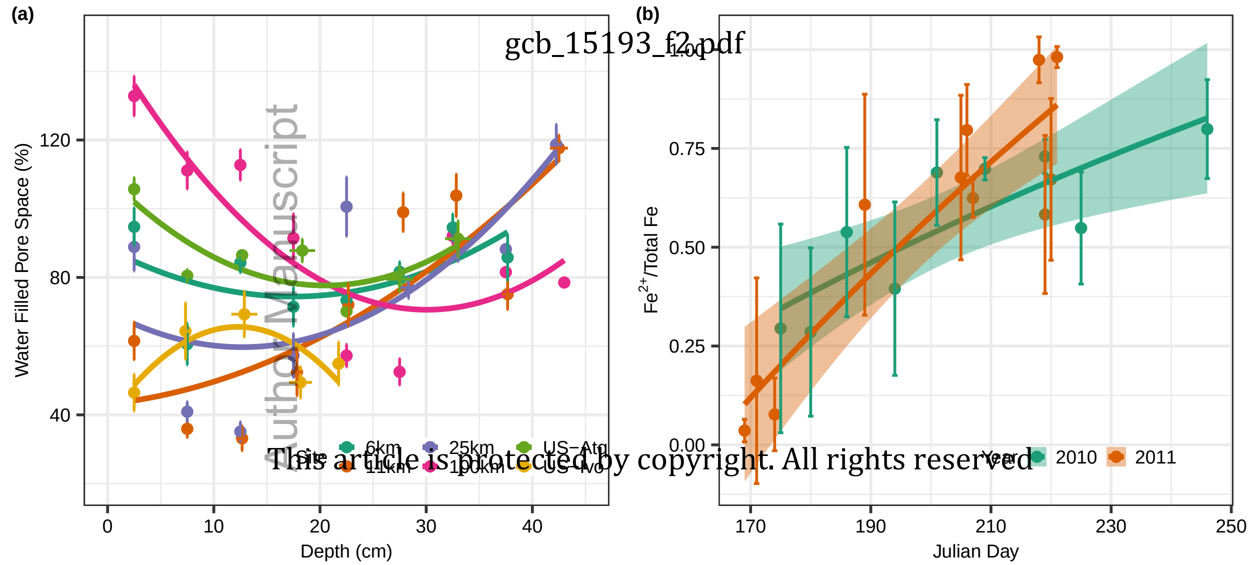

(a)
Water Filled Pore Space (%)
120
80
40
0
10
20
30
40
Depth (cm)
Site
6km
11km
25km
100km
US−Atq
US−Ivo
(b)
Fe2+/Total Fe
1.00
0.75
0.50
0.25
0.00
170
190
210
230
250
Julian Day
Year
2010
2011

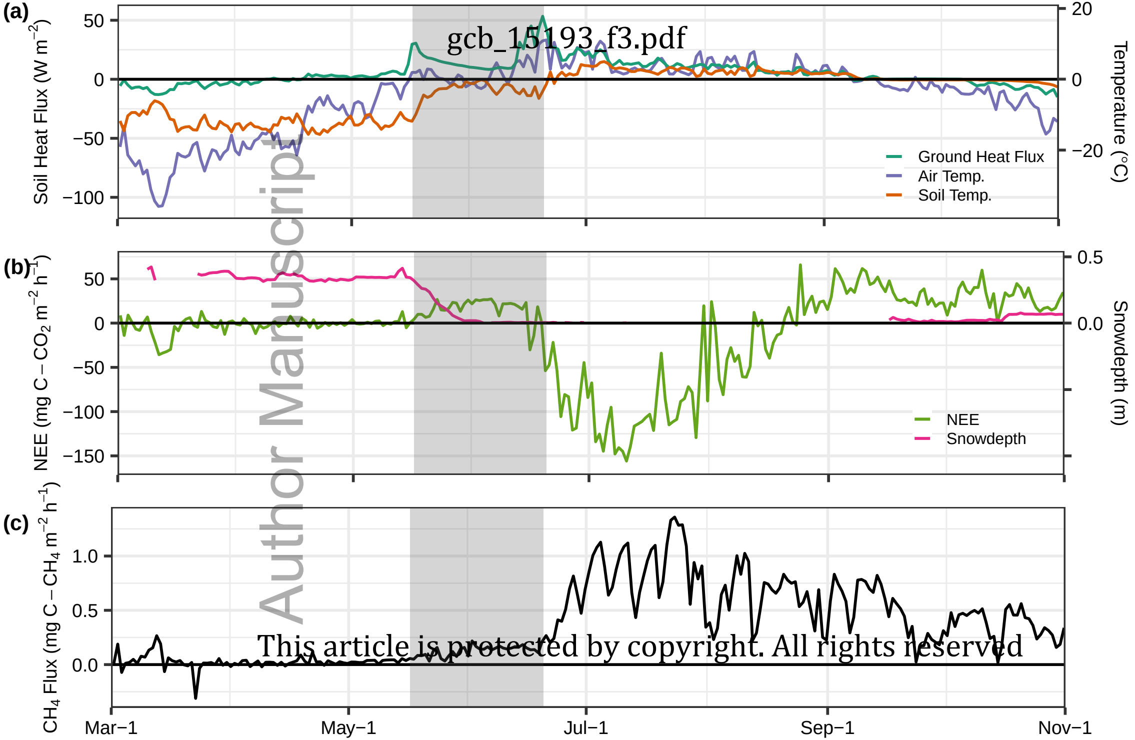
(a)
Soil Heat Flux (W m^{-2})
50
0
−50
−100
Temperature (°C)
20
0
−20
Ground Heat Flux
Air Temp.
Soil Temp.
(b)
NEE (mg C − CO$_2$ m^{-2} h^{-1})
50
0
−50
−100
−150
Snowdepth (m)
0.5
0.0
NEE
Snowdepth
(c)
CH$_4$ Flux (mg C − CH$_4$ m^{-2} h^{-1})
1.0
0.5
0.0
Mar−1
May−1
Jul−1
Sep−1
Nov−1

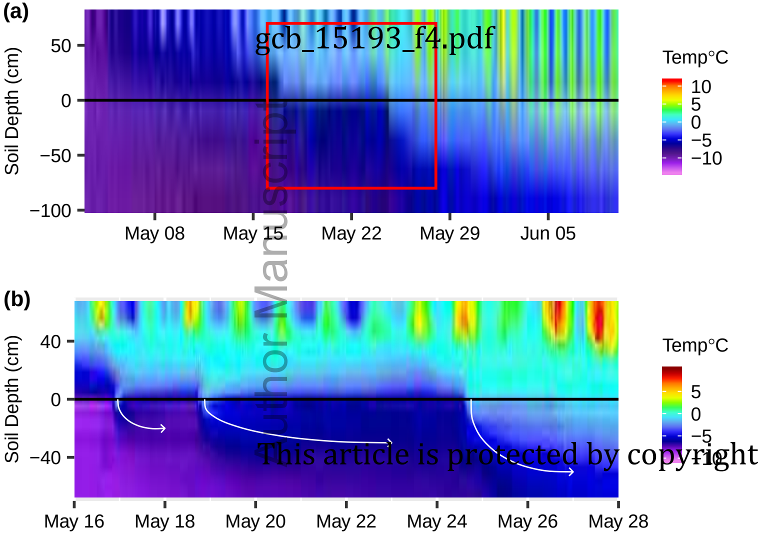

(a)
Soil Depth (cm)
50
0
−50
−100
May 08
May 15
May 22
May 29
Jun 05
Temp°C
10
5
0
−5
−10
(b)
Soil Depth (cm)
40
0
−40
May 16
May 18
May 20
May 22
May 24
May 26
May 28
Temp°C
5
0
−5

gcb_15193_f5.pdf

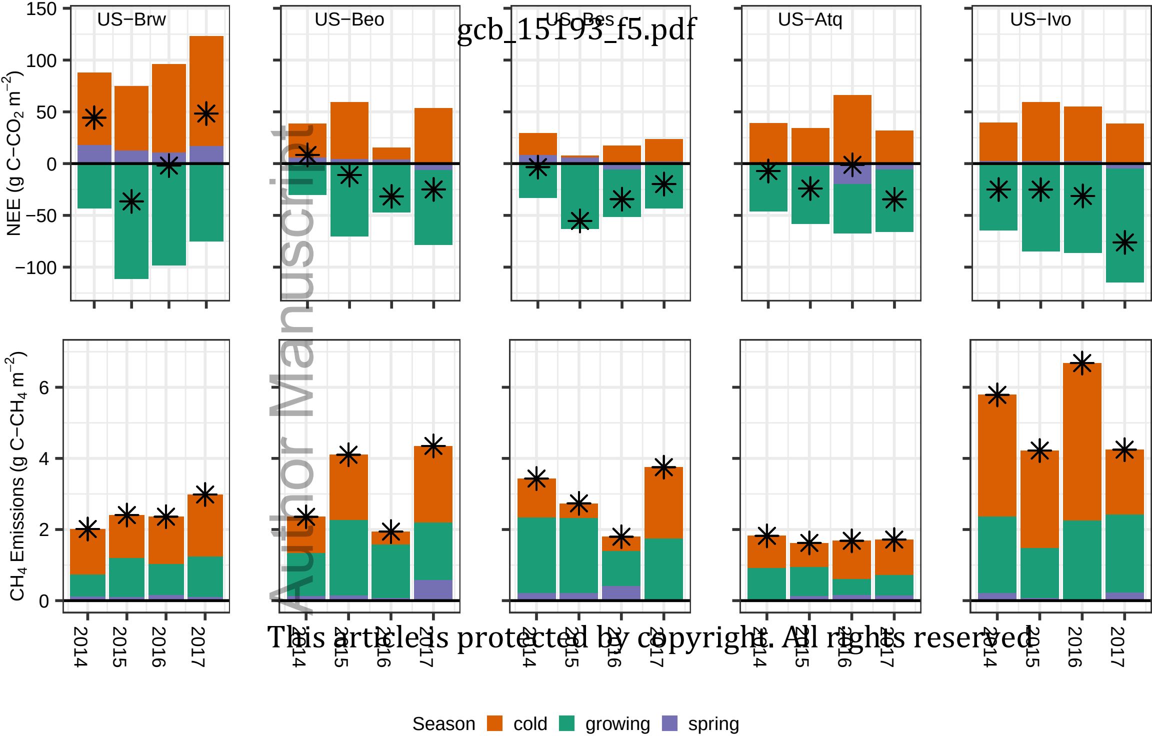

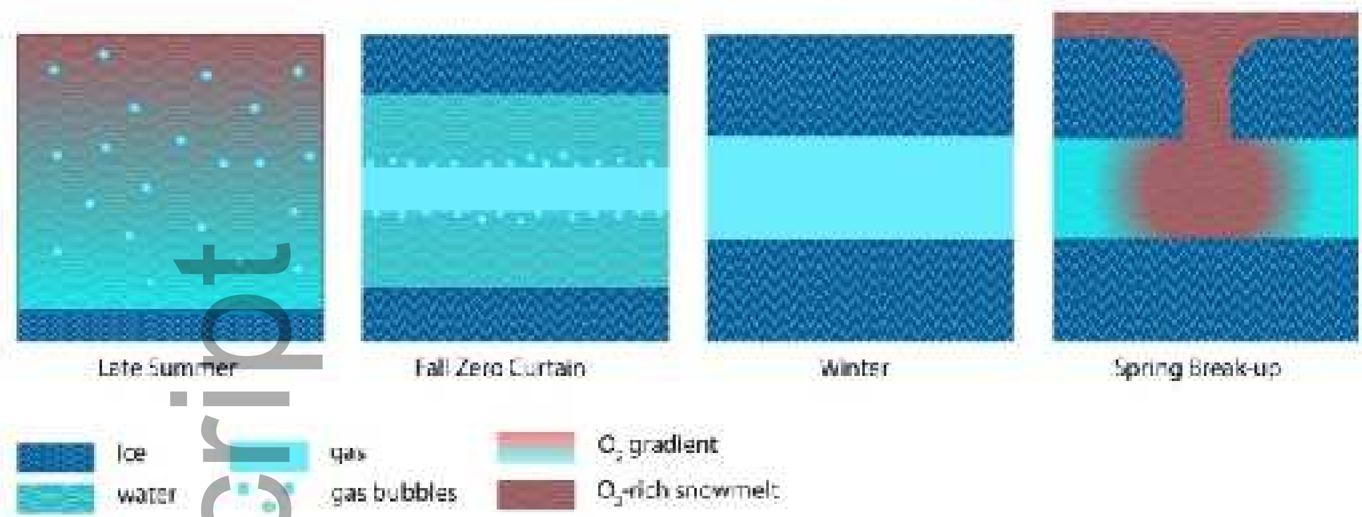

gcb_15193_f6.jpg